LOCV calculation of the equations of state and properties of rapidly rotating neutron stars

A. H. Farajian   M. Bigdeli[1)]   S. Belbasi

Department of Physics, University of Zanjan, Zanjan, 45371-38791, Iran

Abstract: In this paper, we have investigated the structural properties of rotating neutron stars using the numerical RNS code and equations of state which have been calculated within the lowest order constrained variational (LOCV) approach. In order to calculate the equation of state of nuclear matter, we have used UV_{14} +TNI and AV_{18} potentials. We have computed the maximum mass of the neutron star and the corresponding equatorial radius at different angular velocities. We have also computed the structural properties of Keplerian rotating neutron stars for the maximum mass configuration, M_K, R_K, f_K and j_{max}.

Keywords: LOCV method, neutron star matter, equation of state, rotating neutron star

PACS: 21.65.-f, 26.60.Kp, 97.60.Jd   **DOI:** 10.1088/1674-1137/42/6/065102

1   Introduction

All existing studies indicate that observed neutron stars, such as millisecond pulsars (MSPs), are rotating. Recently, many MSPs have been discovered. One of the most rapidly rotating neutron stars is pulsar PSR J1748-2446ad, which has rotational frequency 716 Hz [1]. The rotational frequency f, which can be directly measured, affects the global attributes of neutron stars, specifically, maximum mass, radius, spin parameter and total moment of inertia [2–6]. The maximum mass increases with rotation due to the rotational energy and there are even super-massive sequences [7]. So far, there have been a large number of mass and radii measurements. The accurate measurement of mass for about 35 neutron stars lies in the wide range of $M \sim 1.17-2.0$ $M_\odot$ and the radii of more than a dozen neutron stars lies in the range $R \sim 9.9$–11.2 km [8]. Two well-measured massive neutron stars are MSPs in binary systems, PSR J1614-2230 with mass $M = 1.928 \pm 0.017$ $M_\odot$ [9], and PSR J0348+0432, with mass $M = 2.01 \pm 0.04 M_\odot$ [10]. These massive neutron stars require the equation of state (EOS) of the system to be rather stiff. Present radius determinations are model dependent and subject to large uncertainties. However, some current and planned projects, such as NICER[2)] are trying to determine the radii more precisely. Theoretically, the EOSs have been applied to determine neutron star properties which should be in agreement with the precise observations.

Another important characteristic quantity for compact stars is the dimensionless spin parameter $j \equiv cJ/GM^2$, where J is angular momentum and M is gravitational mass. The astrophysical estimations and implications of j for different astronomical objects have been considered by several authors, e.g. Refs. [11–16]. Török et al. have investigated the mass vs. spin parameter relationship $M(j) = M_0[1+k(j+j^2)]$ for the Z-source Circinus X-1 [15] and atoll source $4U1636-53$ [16]. Kato et al. have shown that a description of the observed correlations of Circinus X-1 requires adopting $M = 1.5-2.0$ $M_\odot$ as the mass of the central star in Circinus X-1 and $j \sim 0.8$ for the dimensionless spin parameter [12]. Recently, this parameter has been studied in detail for uniformly rotating compact stars by Lo and Lin [17]. They have discussed that the spin parameter plays an important role in understanding the observed quasi-periodic oscillations (QPOs) in disk-accreting compact-star systems. They have shown that the maximum value of the spin parameter, j_{max} (spin parameter of a neutron star rotating at the Keplerian frequency), depends on the composition of compact stars. Their results indicate that the value of j_{max} has an upper bound about $j_{max} \sim 0.7$ for traditional neutron stars; and it is independent of the EOS and also insensitive to the mass of the star for $M \geqslant 1M_\odot$ [17]. Their results also indicate that there is no universal upper bound for the spin parameter of quark stars simulated by the MIT bag model and it can be larger than unity ($j_{max} > 1$). A different point of view has been followed by Qi et al. [18]; they have found that the crust structure of compact stars is essential to determine the

maximum value of the spin parameter. They have concluded that when the whole crust EOS is not considered, $j_{\max}$ of compact stars can be larger than 0.7 but also less than 1 for traditional and hyperonic neutron stars and also for hybrid stars, whereas the role of the crust in the total mass of the compact star is negligible. In this paper, we show that only the outer crust structure could play the same roles, see Section 3. Qi et al. also have constructed a universal formula for spin parameter versus frequency, $j=0.48(f/f_k)^3-0.42(f/f_k)^2+0.63(f/f_k)$, for different kinds of compact stars.

In this study, we have investigated the structural properties of rapidly rotating neutron stars with and without outer crust structures. Here we have used EOS for the liquid core of the neutron star which have been calculated within the lowest order constrained variational (LOCV) method with UV_{14} +TNI [19] and AV_{18} [20] potentials. Previously, we used these EOS to determine the core-crust transition parameters and global attributes of core and crust for neutron stars [21].

2   Neutron star matter equation of state

We have employed the EOS for neutron star matter by describing the neutron star's outer crust, inner crust and the liquid core. For the inner crust, we use the EOS which is calculated by Douchin and Haensel [22], and for the outer crust, the Baym-Pethick-Sutherland EOS [23] is used. In the case of the neutron star core, we assume a charged neutral infinite system which is a mixture of leptons and interacting nucleons. The energy density of this system can be obtained as follows,

$$\varepsilon=\varepsilon_N+\varepsilon_l, \tag{1}$$

where ε_N (ε_l) is the energy density of nucleons (leptons). The energy density of leptons, which are considered as a noninteracting Fermi gas, is given by,

$$\varepsilon_{lep} = \sum_{l=e,\ \mu}\ \sum_{k\leqslant k_l^F}(m_l^2c^4+\hbar^2c^2k^2)^{1/2} \ . \tag{2}$$

In this equation, $k_l^F=(3\pi^2\rho_l)^{1/3}$ is the Fermi momentum of leptons. The nucleon contribution of energy density is given by,

$$\varepsilon_N=\rho(E_{\mathrm{nucl}}+m_Nc^2), \tag{3}$$

where E_{nucl} is the total energy per particle of asymmetric nuclear matter and ρ is the total number density,

$$\rho=\rho_p+\rho_n.$$

Here, ρ_n and ρ_p are number density of neutrons and protons respectively.

The β-equilibrium conditions and charge neutrality of neutron star matter impose the following coupled constraints on our calculations,

$$\mu_e=\mu_\mu = \mu_n-\mu_p \tag{4}$$

$$\rho_p=\rho_e+\rho_\mu. \tag{5}$$

We find the abundance of the particles by solving these coupled equations and calculate the total energy and the EOS of the neutron star matter.

In the following, we determine the energy per particle of asymmetric nuclear matter, E_{nucl}, in more detail by using the LOCV method. In our formalism, the energy per particle is written in terms of correlation function, f, and its derivatives; and approximately given up to the two-body term as the following form [24],

$$E_{\mathrm{nucl}}([f]) = \frac{1}{A}\frac{\langle\psi|H|\psi\rangle}{\langle\psi|\psi\rangle}=\frac{1}{A}\sum_{\tau=n,p}\sum_{k\leqslant k_\tau^F}\frac{\hbar^2k^2}{2m_\tau}$$
$$+\frac{1}{2A}\sum_{ij}\langle ij|\nu(12)|ij\rangle_a, \tag{6}$$

where $\psi=\mathcal{F}\phi$ is a trial many-body wave function. Here ϕ is the Slater determinant of wave function of A independent nucleons and $\mathcal{F}=\mathcal{S}\prod_{i>j}f(ij)$ ($\mathcal{S}$ is a symmetrizing operator) is a Jastrow form of A-body correlation operator. In the above equation, $k_\tau^F = (3\pi^2\rho_\tau)^{1/3}$ is the Fermi momentum of nucleons and $\nu(12)$ is the effective potential, which is given by,

$$\nu(12)=-\frac{\hbar^2}{2m}[f(12),[\nabla_{12}^2,f(12)]]+f(12)V(12)f(12). \tag{7}$$

Here, $f(12)$ and $V(12)$ are the two-body correlation and potential, respectively. In our calculations, we used the UV_{14} +TNI and AV_{18} two-body potentials.

In this formalism, the correlation function is considered as different forms [25], and calculated by numerically solving of set of coupled and uncoupled Euler-Lagrange differential equations [26]. These differential equations are a result of functional minimization of the two-body cluster energy with respect to the correlation functions variation. For more details see Refs. [26–29].

A summary of our results for bulk properties of symmetric nuclear matter for the UV_{14} +TNI and AV_{18} potentials are given in Table 1. In this table, we have given the saturation density ρ_s, and the corresponding values of energy per particle E_0, incompressibility K_0, and nuclear symmetry energy S_0. The calculated saturation properties of symmetric nuclear matter are in excellent agreement with the experimental data [30] for the UV_{14} +TNI potential.

Table 1.   Saturation density and corresponding values of energy per particle, incompressibility and symmetry energy of symmetric nuclear matter. Here ρ_s is given in fm^{-3} and energy parameters are in MeV.

potential	ρ_s	E_0	K_0	S_0
UV_{14} + TNI	0.17	-16.86	261	31.27
AV_{18}	0.31	-18.47	301	36.24

The pressure of neutron star matter can be calculated by the following relation,

$$P = \rho \frac{\partial \varepsilon}{\partial \rho} - \varepsilon. \qquad (8)$$

In Fig. 1, we have plotted the pressure of neutron star matter at the core of the star for the mentioned potentials versus total energy density. In this figure we also show the EOS for outer and inner crust. It is seen that the UV_{14} +TNI potential leads to a stiffer EOS.
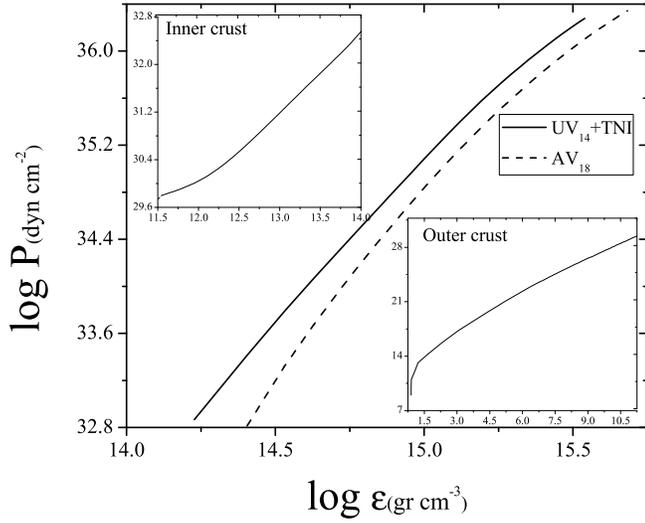
Fig. 1.   The EOS of neutron star matter for the UV_{14} + TNI and AV_{18} potentials. The EOS of the outer and inner crust are also shown.

3   Results and discussion

We now proceed to show our results for rotating neutron stars. We make use of the numerical RNS code (http://www.gravity.phys.uwm.edu/rns/), which integrates the Einstein field equations for a rapidly rotating neutron star given a perfect fluid EOS [31]. In Fig. 2, we show the gravitational mass versus (circumferential) radius for two different microscopic EOS at fixed frequency $f = 0$ and $f = 716$ Hz. The solid (dashed) curve shows the result for neutron stars including (excluding) the outer crust structure. Clearly, the inclusion of the outer crust has no considerable effect on the maximum mass and corresponding radius of the neutron star. However, the global structure of the neutron star is sensitive to its angular velocity, and the maximum mass increases by increasing the rotation velocity.

From this figure, one can compare the results of the EOS derived using the UV_{14}+TNI and AV_{18} potentials. At a frequency of $f = 716$ Hz, which corresponds to the spin period $P \approx 1.39$ ms, by applying the AV_{18} potential, we get $M_{\max}/M_{\odot} \simeq 1.653$ ($\simeq 1.649$) for a neutron star with (without) outer crust structure. Using

the UV_{14} +TNI leads to larger stellar mass and radius in comparison with the AV_{18} potential, and we obtain $M_{\max}/M_{\odot} \simeq 2.0278$ ($\simeq 2.0275$) with the UV_{14} +TNI potential. This is in good agreement with the results obtained by observations for the millisecond pulsar PSR J0348+0432, $M = 2.01 \pm 0.04 M_{\odot}$ [10]. However, this pulsar rotates with the lower frequency of $\simeq 25$ Hz. This does not affect the good comparison, because in this frequency range the maximum mass has a little variance with the rotation (see Fig. 2 and Table 2).
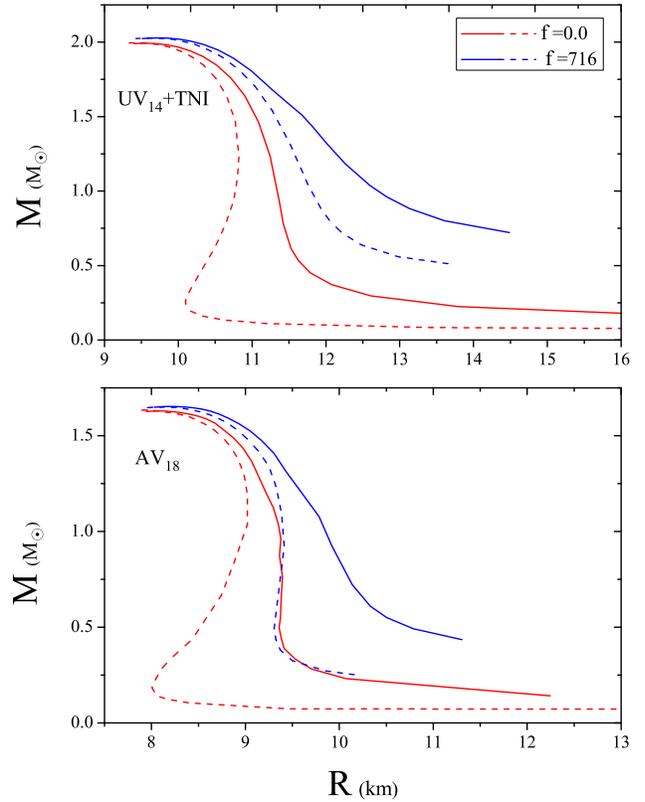
Fig. 2.   (color online) The gravitational mass (M) versus circumferential radius (R) for non-rotating and rotating neutron star with the UV_{14} +TNI and AV_{18} potentials. The frequency (f) is given in Hz. The solid (dashed) curve shows the result for neutron stars including (excluding) the outer crust structure.

Another crucial parameter that can be used to describe rotating neutron stars is the Keplerian frequency, f_k, the maximum value of frequency. We have plotted Keplerian frequencies versus gravitational masses in Fig. 3. It is seen that f_k depends on the EOS models presented here. From Fig. 3, for the case of the UV_{14} +TNI potential, we find that the value of the Keplerian mass corresponding to our calculated frequency, $f_k \simeq 1.93$ kHz ($f_k \simeq 1.96$ kHz) is about $M_k \simeq 2.36 M_{\odot}$ ($M_k \simeq 2.40 M_{\odot}$) for a neutron star with (without) outer crust structure. For the case of the AV_{18} potential, we find $M_k \simeq 1.95 M_{\odot}$

($M_k \simeq 1.98 M_\odot$) corresponding to $f_k \simeq 2.23$ kHz ($f_k \simeq 2.24$ kHz). It is seen that the Keplerian mass and frequency for a neutron star with outer crust are a little lower than those of a neutron star without outer crust.
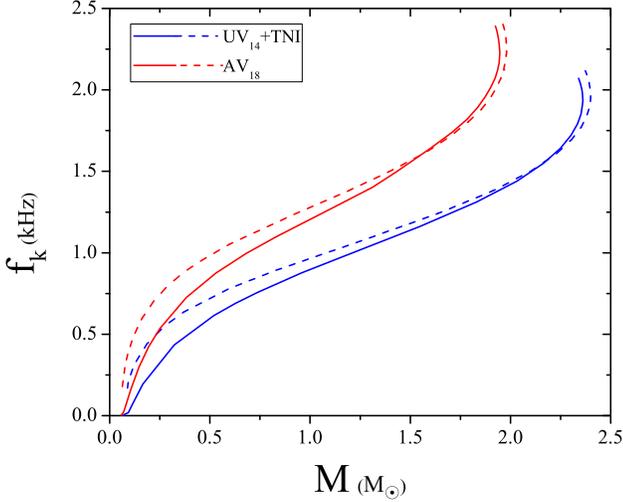
Fig. 3.   (color online) The variation of the Keplerian frequency (f_K) with gravitational mass M for neutron stars with (solid curve) and without (dashed curve) outer crust structure.
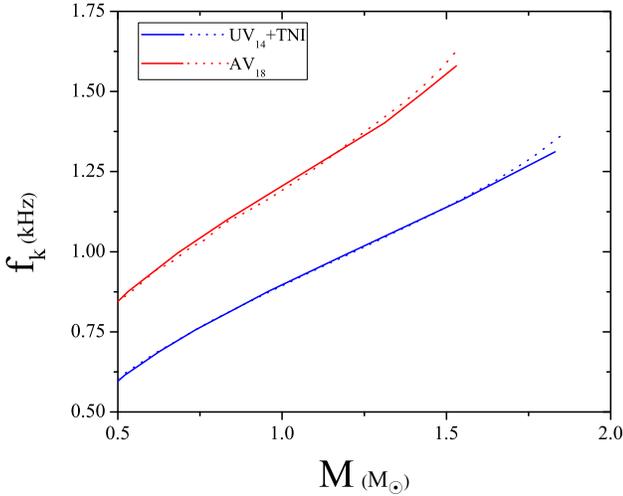
Fig. 4.   (color online) The variation of the Keplerian frequency (f_K) with gravitational mass M for neutron stars for precise values of Keplerian frequency (solid curve) and those given by Eq. (9) (dotted curve).

We have also calculated Keplerian frequency using the fit formula proposed by Haensel et al. [6],

$$f_K = 1.08 \text{ kHz} \left(\frac{M}{M_\odot} \right)^{1/2} \left(\frac{R}{10 \text{ km}} \right)^{-3/2}, \qquad (9)$$

where $0.5 M_\odot \leqslant M \leqslant 0.9 M_{\max}^{stat}$, $M_{\max}^{stat}$ is the maximum mass of the non-rotating (static) configuration and R

is the corresponding radius. The results are shown in Fig. 4. As can be seen from this figure, there is a good agreement between the precise values and those calculated using the above equation, especially for the UV_{14} +TNI potential.

In the following, we discuss the relation between maximum mass and frequency in more detail. In Fig. 5, we present the maximum mass in units of Keplerian mass, $M_{\max}(M_K)$, as a function of stellar frequency in units of Keplerian frequency, $f(f_K)$. This figure shows that for both EOS employed in the present work, $M_{\max}(M_K)$ displays a similar behavior versus $f(f_K)$ and, nearly, does not depend on the EOS. According to this behavior, we find

$$0.835 M_K \lesssim M_{\max} \leqslant 1.0 M_K.$$

In other words, the maximum mass in the Keplerian configuration increases about 20% compared to the maximum mass of non-rotating configurations. This result is in agreement with those obtained by the universal relation $M_k \simeq (1.203 \pm 0.022) M_{\max}^{stat}$ proposed by Breu and Rezzola [32].
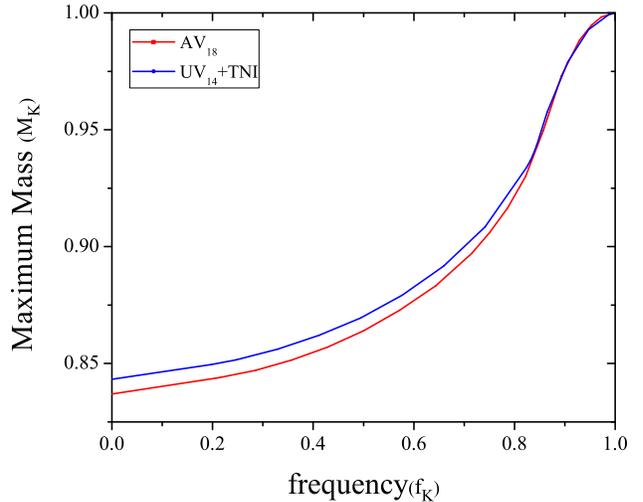
Fig. 5.   (color online) The maximum mass versus frequency for different equations of state. The maximum mass and frequency are given in units of Keplerian mass and frequency, respectively.

Now, we focus on the treatment of the dimensionless spin parameter j, for rotating neutron stars. Here, we would like to consider the influence of the outer crust structure on the spin parameter at Keplerian frequency, i.e. maximum spin parameter, $j_{\max}$. In order to achieve this, we shown the maximal spin parameter, $j_{\max}$, as a function of gravitational mass in Fig. 6. As can be seen from this figure, the maximal spin parameter of the rotating neutron star displays different behaviors when we either include or exclude the outer crust structure. It is seen that $j_{\max}$ for NSs with the outer crust structure lying in the narrow range $\sim$ (0.64 - 0.7) for $M \geqslant 0.5 M_\odot$.

Therefore, we see that our result for the upper limit of $j_{max}(\leqslant 0.7)$ is in agreement with those reported earlier [17, 18] for traditional neutron stars, while, for the neutron star with only inner crust structure j_{max} is larger than 0.7 and this value is the lower limit of $j_{max}(\geqslant 0.7)$. This shows that, in spite of the role of outer crust structure in the maximal mass, its role in maximal spin parameter is important. It is worth noting that the similar results have been concluded in the work by Qi et al., but they have considered the whole crust structure in calculating the maximum value of the spin parameter [18].
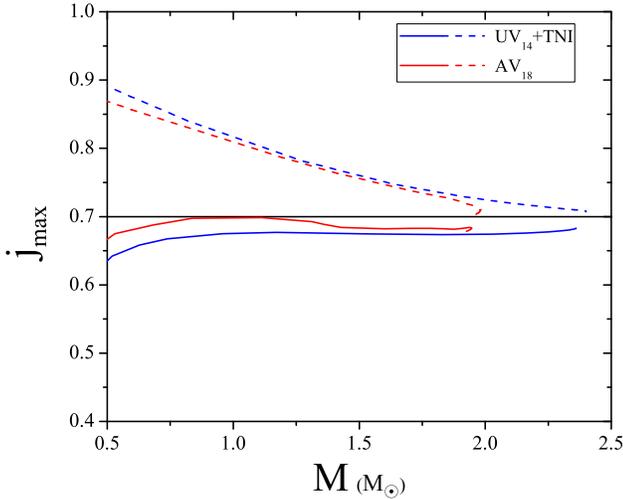
Fig. 6. (color online) The variation of the maximum spin parameter (j_{max}) with gravitational mass M for neutron stars with (solid curve) and without (dashed curve) outer crust structure.

Finally, we have investigated the spin parameter, j, of slow rotating neutron stars. In Fig. 7, we plot the spin parameter j as a function of the rotational frequency normalized to Keplerian frequency, f/f_k, for using the UV_{14}+TNI at different values of baryonic mass of neutron star, $M_b/M_\odot = 1, 1.5, 2$.

It is seen that for each fixed frequency, the curves are essentially independent of mass sequence. A unified relationship could be fitted approximately by the formula $j = 0.16(f/f_k)^3 - 0.1(f/f_k)^2 + 0.612(f/f_k)$, as denoted by the circles. We also show the result of the universal formula $j = 0.48(f/f_k)^3 - 0.42(f/f_k)^2 + 0.63(f/f_k)$, which has been suggested in Ref. [18], with squares, for comparison.

A summary of our results for the structural properties of rotating neutron stars with and without outer crust predicted from different EOS is given in Table 2. This table also includes the maximum mass and corresponding equatorial radius for neutron stars at $f = 0$, and 716 Hz, as well as the structural properties of Keplerian rotating neutron stars for the maximum mass configuration, M_K, R_K, f_K and j_{max}.
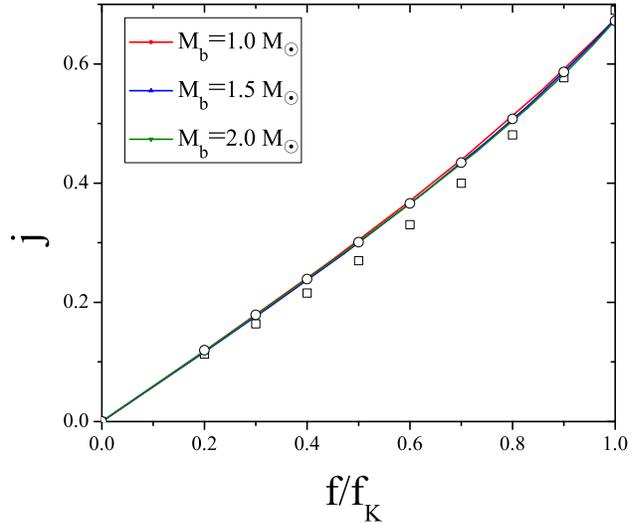
Fig. 7. (color online) The dimensionless spin parameter (j) as a function of the rotational frequency normalized to Keplerian frequency (f/f_K) for the UV_{14}+TNI potential. The circles show our fitted formula, and squares that from Ref. [18].

Table 2. Maximum mass and corresponding equatorial radius for neutron stars at $f = 0$, 716 Hz. The structural properties of Keplerian rotating neutron stars for maximum mass configuration, M_K, R_K, f_K and j_{max} are also given. The gravitational mass is given in solar masses ($M_\odot$), R is in km and f_K in kHz. The quantities in parenthesis show the results of our calculation for neutron stars without outer crust structure.

potential	$M_{f=0}$	$R_{f=0}$	$M_{f=716}$	$R_{f=716}$	M_K	R_K	f_K	j_{max}
UV_{14} + TNI	1.99(1.99)	9.67(9.56)	2.027(2.027)	9.8(9.7)	2.36(2.40)	12.59(12.59)	1.93(1.96)	0.682(0.707)
AV_{18}	1.63(1.63)	8.09(7.92)	1.653(1.649)	8.22(8.11)	1.95(1.98)	10.77(10.82)	2.23(2.24)	0.683(0.71)

4   Summary and conclusions

In this work, we have calculated the structural properties of rotating neutron stars with and without outer

crust structures. Here we have employed lowest order constrained variational approach and used the UV_{14} +TNI and AV_{18} potentials to compute the EOS of nuclear matter. We have computed maximum mass and

corresponding equatorial radius at fixed frequency $f=0$ and $f=716$ Hz. We have also computed the structural properties of Keplerian rotating neutron stars for maximum mass configuration, M_K, R_K, f_K and j_{max}.

A summary of our results for the structural properties of rotating neutron stars with and without outer crust predicted from different EOS is given in Table 2. Our results show that the maximal spin parameter, j_{max}, lies in the narrow range $\sim (0.64 - 0.7)$ for $M \geqslant 0.5 M_\odot$ for the EOS considered. In the case of slow rotating neutron stars, we have suggested a unified relationship for the spin parameter $j=0.16(f/f_k)^3-0.1(f/f_k)^2+0.612(f/f_k)$ which is essentially independent of mass sequence. Finally, our results in the Keplerian configuration are in very good agreement with those of other studies.

References

1 J. W. T. Hessels et al, Science, **311**: 1901 (2006)
2 J. B. Hartle, and K. S. Thorne, ApJ, **153**: 807 (1968)
3 N. Stergioulas, and J.L. Friedman, ApJ, **444**: 306 (1995)
4 M. Salgado, S. Bonazzola, E. Gourgoulhon, and P. Haensel, Astron. Astrophys, **108**: 455 (1994)
5 G. B. Cook, S. L. Shapiro, and S. A. Teukolsky, ApJ, **424**: 823 (1994)
6 P. Haensel, J. L. Zdunik, M. Bejger, and J. M. Lattimer, Astron. Astrophys, **502**: 605 (2009)
7 M. Salgado, S. Bonazzola, E. Gourgoulhon, and P. Haensel, Astron. Astrophys, **291**: 155 (1994)
8 F. Özel, and P. Freire, Annu. Rev. Astron. Astrophys, **54**: 401 (2016)
9 P. B. Demorest, T. Pennucci, S. M. Ransom, M. S. E. Roberts, and J. W. T. Hessels, Nature, **467**: 1081 (2010)
10 J. Antoniadis et al, Science, **340**: 448 (2013)
11 M. D. Duez, S. L. Shapiro, and H. J. Yo, Phys. Rev. D, **69**: 104016 (2004)
12 S. Kato, Publ. Astron. Soc. Japan, **60**: 889 (2008)
13 T. Piran, Rev. Mod. Phys, **76**: 1143 (2005)
14 M. Shibata, Phys. Rev. D, **67**: 024033 (2003); M. Shibata, ApJ, **595**: 992 (2003)
15 G. Török, P. Bakala, E. Srámková, Z. Stuchlik, and M. Urbanec, ApJ, **714**: 748 (2010)
16 G. Török, P. Bakala, E. Srámková, Z. Stuchlik, and M. Urbanec, and K. Goluchová, ApJ, **760**: 138 (2012)
17 K. W. Lo and L. M. Lin, ApJ, **728**: 12 (2011)
18 B. Qi, N. B. Zhang, B. Y. Sun, S. Y. Wang, and J. H. Gao, RAA, **16**, No. 4 (2016)
19 I. E. Lagaris and V. R. Pandharipande, Nucl. Phys. A, **359**: 349 (1981)
20 R. B. Wiringa, V. G. J. Stoks, and R. Schiavilla, Phys. Rev. C, **51**: 38 (1995)
21 M. Bigdeli, and S. Elyasi, Eur. Phys. J. A, **51**: 38 (2015)
22 F. Douchin, and P. Haensel, Astron. Astrophys, **380**: 151 (2001)
23 G. Baym, C. Pethick, and D. Sutherland, ApJ, **170**: 299 (1971)
24 J. W. Clark and N. C. Chao, Lettere Nuovo Cimento, **2**: 185 (1968)
25 J. C. Owen, R. F.Bishop, and J. M. Irvine, Nucl. Phys. A, **277**: 45 (1997)
26 G. H. Bordbar and M. Modarres, Phys. Rev. C, **57**: 714 (1998)
27 M. Modarres, and G. H. Bordbar, Phys. Rev. C, **58**: 2781 (1998)
28 M. Bigdeli, G. H. Bordbar, and A. Poostforush, Phys. Rev. C, **82**: 034309 (2010)
29 M. Bigdeli, Phys. Rev. C, **82**: 054312 (2010)
30 P. E. Haustein, At. Data Nucl. Data Tables, **39**: 185 (1988)
31 N. Stergioulas, Living Rev. Rel., **6**: 3 (2003)
32 C. Breu and L. Rezzola, MNRAS, **459**: 646 (2016)